Strain and Temperature Sensors Using Multimode Optical Fiber Bragg Gratings and Correlation Signal Processing

Jirapong Lim, Qingping Yang, Barry E. Jones, and Phillip R. Jackson

***Abstract*—Multimode fiber optic Bragg grating sensors for strain and temperature measurements using correlation signal processing methods have been developed. Two multimode Bragg grating sensors were fabricated in 62/125 μm graded-index silica multimode fiber; the first sensor was produced by the holographic method and the second sensor by the phase mask technique. The sensors have signal reflectivity of approximately 35% at peak wavelengths of 835 nm and 859 nm, respectively.**

Strain testing of both sensors has been done from 0 to 1000 $\mu\varepsilon$ and the temperature testing from −40 to 80 °C. Strain and temperature sensitivity values are 0.55 pm/$\mu\varepsilon$ and 6 pm/°C, respectively. The sensors are being applied in a power-by-light hydraulic valve monitoring system.

***Index Terms*—Bragg grating, correlation, hydraulic valve, multimode, optical fiber, optically-powered, strain, temperature.**

I. Introduction

DURING the past decade, single-mode optical fiber Bragg gratings (SM-FBGs) have been used for strain and temperature sensing in many applications such as structural monitoring, down-hole and hazardous environments. Recent research work has been reported on a differential-pressure (DP) flow sensor using SM-FBGs for hydraulic valve monitoring applications [1]. However, using SM-FBGs in the application of an optically-powered hydraulic valve monitoring system is not really appropriate [2], [3]. This is because the system must utilize only one optical fiber for both optical power transmission and for sensing. The optical fiber transmits power from a laser source into the optically powered hydraulic valve at the remote end of the fiber. It is also used for feeding the valve operation information back to the valve monitoring system via the same fiber, as shown in Fig. 1; the optical fiber link might be 4 km in length. The other reason is that it is difficult to launch high optical power into the single-mode optical fiber due to its small core diameter. Therefore, a multimode optical fiber Bragg grating (MM-FBG) is more suitable due to its larger core diameter. A particular advantage of this configuration is that no optical fiber coupler is required at the valve end, and this makes the system less complex and minimizes optical power loss.

Manuscript received May 29, 2001; revised May 2, 2002. This work was supported in part by a Ph.D. scholarship from The Royal Thai Government and by Flight Refuelling Ltd., Dorset, U.K.

J. Lim is with the King Mongkut's Institute of Technology, North Bangkok, Thailand.

Q. Yang and B. E. Jones are with the Brunel Centre for Manufacturing Metrology, Brunel University, Uxbridge, Middlesex, U.K.

P. R. Jackson is with Flight Refuelling Ltd., Wimborne, Dorset, U.K.

Digital Object Identifier 10.1109/TIM.2002.802253

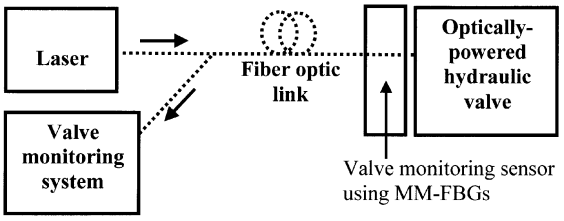

Fig. 1. Optically powered hydraulic valve system.

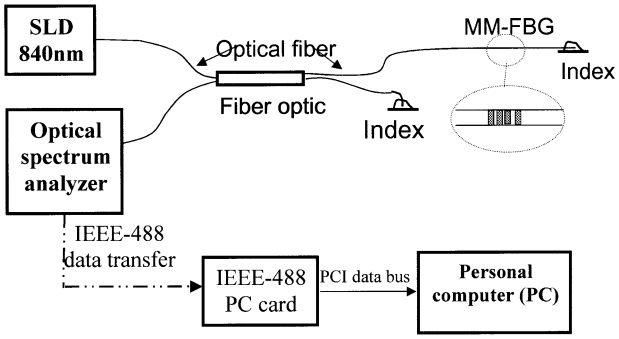

Fig. 2. Experimental setup.

The early use of MM-FBGs was reported by Wanser *et al.* [4], [5]. Microbending was used to disturb the mode population in an optical fiber through mode coupling before passing the light to the MM-FBG. A similar approach using the bending effect on a transmission spectrum of the MM-FBG for displacement sensing was introduced by Mizunami *et al.* [6], [7]. However, these sensing techniques require mechanical parts and are therefore more complicated than conventional SM-FBGs. The use of MM-FBGs for both strain and temperature sensing by using the same method as used with a Bragg grating in a single-mode fiber is also possible [8], [11].

Changes in optical signals obtained from a multimode optical fiber can be caused by changes in both strain and temperature. Significant variation in these signals can be noticed from the amplitude-wavelength signature by number of peaks, peak values and signal distortions, but it is difficult to pinpoint the amount of wavelength shift that is proportional to strain or temperature changes.

In this paper, a method of using correlation signal processing to quantify variation of wavelength shift caused by altering strain or temperature is reported. Advantages of using this method include minimizing the effect of variation in signal amplitude and shape of the MM-FBG amplitude wavelength spectrum, and reducing the effect of noise. Tests have been

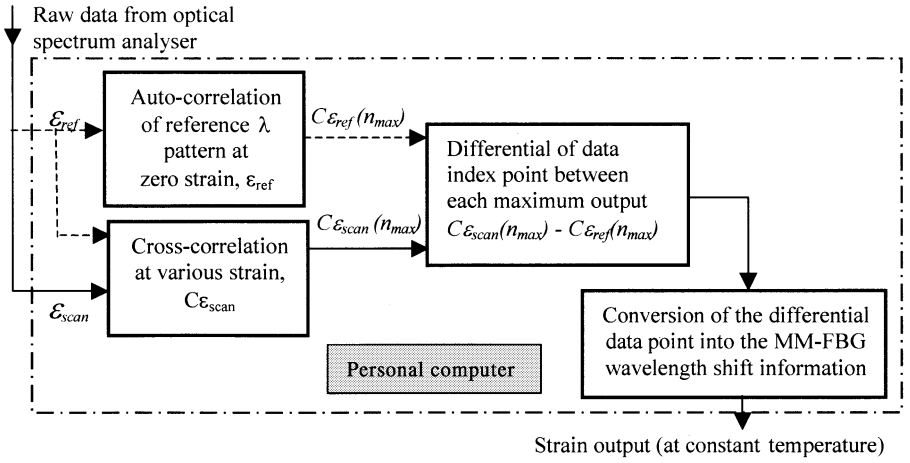

(a)

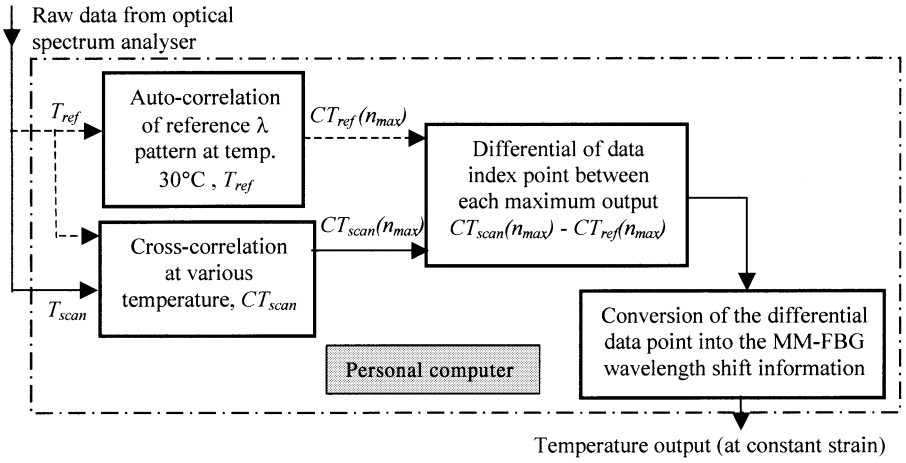

(b)

Fig. 3. Signal processing scheme for (a) strain test and (b) temperature test.

performed to compare the characteristics of the two MM-FBG sensors for axial strain measurement and for the temperature measurement. The effect of temperature on strain sensing has also been investigated.

II. Basic Scheme

Two MM-FBGs fabricated in 62.5/125 μm graded-index silica multimode fiber have been tested using the same experimental setup (Fig. 2). The first MM-FBG was fabricated by the holographic technique without buffer coating, while the second MM-FBG sensor was fabricated by the phase mask technique with acrylate buffer recoating. The reflectivity of the first and second MM-FBGs is approximately 35% at peak wavelength of 835 and 859 nm, respectively. In the experimental setup, one end of the MM-FBG was connected to one of the output fibers of a 50:50, 2×2 multimode optical fiber coupler. The other end of the MM-FBG and the output end of the coupler were placed in index matching gel. At the input end of the coupler, one optical fiber was connected to a light source and the other optical fiber fed a sensing signal to an optical spectrum analyzer (Anritsu MS99A). The spectrum of the reflected signal from a Bragg grating in a multimode optical fiber is very different for different light sources [7]. For example, using a halogen lamp high multimode excitation occurs, and this results in more multiple peaks and a wider spectrum of reflected signal than occurs for the lower order mode excitation light sources such as laser diode, LED, and super-luminescent diode (SLD). For graded-index MM-FBGs, the propagation constant for the Nth principal mode can be approximated by the equation [7]

$$\beta = \frac{2\pi}{\lambda} \cdot n_1 \sqrt{1 - 4\Delta \frac{N+1}{V}} \tag{1}$$

where β is the propagation constant at the phase-matching condition $\beta = \pi/\Lambda$, Λ the grating period, λ the Bragg wavelength, n_1 refractive index of the core, V normalized frequency ($V = 2\pi a \cdot NA/\lambda$), a the fiber core radius, NA the fiber numerical aperture, and Δ the maximum relative index difference between core and cladding of the fiber. To achieve a low complexity of MM-FBG signal, the SLD with a single-mode optical fiber pigtail, providing 0.5 mW of light power at wavelength 849 nm, was selected for the experiments.

To investigate the strain characteristic, axial strain was applied to the fiber using a fiber fixture/drawer. The axial strain was varied from 0 to 1000 $\mu\varepsilon$ by adjusting an accurate micrometer. The strain characteristic for the first-order mode of the MM-FBG is similar to that in a conventional SM-FBG strain

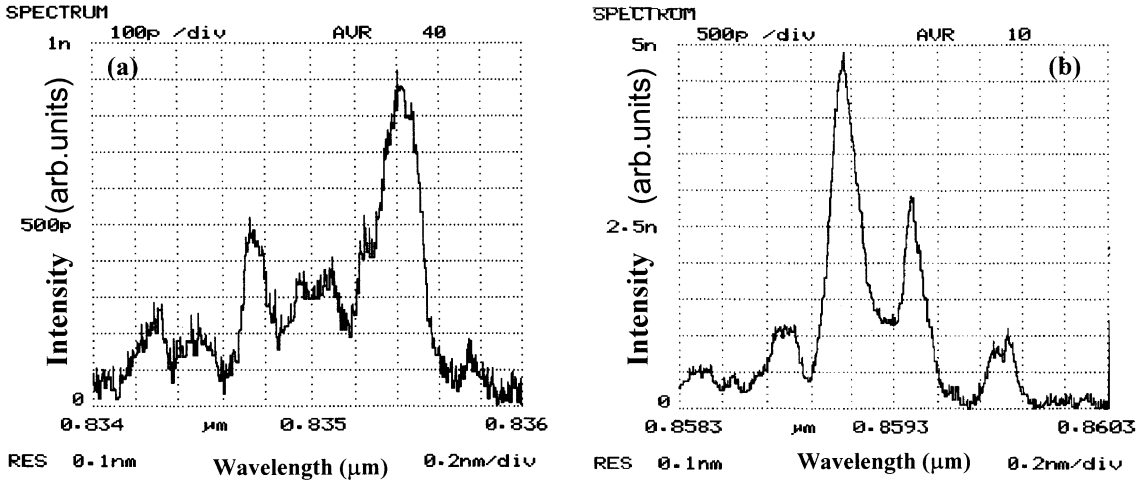

(a) (b)

Fig. 4. The multimode FBG spectrum of (a) the first FBG and (b) the second FBG, with zero strain at room temperature.

sensor [8]. The Bragg grating resonance peak wavelength shift λ_B may be expressed by the Bragg equation [8]–[11]

$$\Delta\lambda_B = (1 - P_e)\lambda_B \cdot \varepsilon \tag{2}$$

where $\Delta\lambda_B$ is the Bragg grating wavelength shift, ε the applied strain, p_e the effective photoelastic coefficient (≈ 0.22), and λ_B the Bragg grating center wavelength.

The thermally induced shift in the FBG is caused by variation in the period of the grating and by variations in the reflective index of the core and cladding. Temperature dependence of the MM-FBGs can be estimated from a complex mathematical model [6]

$$\frac{d\lambda}{dT} = \frac{\lambda^2}{dn_1\Lambda^2} \cdot \frac{d\Lambda}{dT} + \left[\frac{\lambda^2}{2n_1^2\Lambda} - \frac{\lambda^2(N+1)(3n_2 - 2n_1)}{2\pi a n_1^2\sqrt{2n_1(n_1 - n_2)}}\right] \cdot \frac{dn_1}{dt} + \frac{\lambda^2(N+1)}{2\pi a n_1\sqrt{2n_1(n_1 - n_2)}} \cdot \frac{dn_2}{dT} \tag{3}$$

where n_1 is the refractive index of the core, n_2 the refractive index of the cladding, a the fiber core radius, Λ the grating period, and λ the FBG wavelength. The dn_1/dT for silica core and dn_2/dT for silica cladding of the fiber have a value $1 \times 10^{-5}/^{\circ}$C. The thermal expansion coefficient $\alpha = (d\Lambda/dT)$ has a small value of 0.55×10^{-6}. A temperature test has been performed by placing the MM-FBG in a temperature-controlled chamber; the temperature was varied between -40 and 80 °C.

For the signal-processing scheme, a personal computer (PC) with data-acquisition software has been employed to control and correct data from the optical spectrum analyzer obtained via an IEEE-488 data bus. The signal acquisition takes about 2 s, and the autocorrelation and cross-correlation signal processing used to analyze the data from the MM-FBG can be done in less than 1 s by using a special signal-processing feature in the software. The cross-correlation $r_{12}(n)$ between two data sequences each containing N data points can be written as [12]

$$r_{12}(n) = \frac{1}{N}\sum_{n=0}^{N-1} x_1(n)x_2(n) \tag{4}$$

where $x_1(n)$ is the first data sequence and $x_2(n)$ the second data sequence. The result of correlation is solely dependent on the number of data points (400 points for the spectrum analyzer used).

Data processing for the strain measurement is performed by processing the MM-FBG spectrum (scanned by the optical spectrum analyzer), initially using zero strain, to provide a reference pattern ε_{ref}. The raw reference data is kept in the memory of the PC and is processed by the autocorrelation method [Fig. 3(a)]. The output from the auto-correlation is used for the correlation strain reference $C\varepsilon_{\text{ref}}$, and this is also put into the PC memory. Then, scanning data is processed for a particular value of applied strain. This strain data $\varepsilon_{\text{scan}}$ is processed by doing the cross-correlation with the reference data ε_{ref}. The result of the cross-correlation $C\varepsilon_{\text{scan}}$ is used to compare with the correlation strain reference $C\varepsilon_{\text{ref}}$. The distance between maximum points of each result, $C\varepsilon_{\text{scan}}(n_{\max}) - C\varepsilon_{\text{ref}}(n_{\max})$ (where $n_{\max}$ is the data index number point at the maximum value of a correlation result) can be converted into the MM-FBG wavelength shift information. The information from the temperature-dependent test has been investigated using the same method [Fig. 3(b)]. The reference signal pattern, T_{ref}, for the temperature test was set at a temperature of 30 °C.

III. Results

The reflected spectra of both MM-FBGs with zero strain at room temperature are shown in Fig. 4(a), the holographic MM-FBG, and (b), the phase-mask MM-FBG. Six propagation modes can be implied by noticing the number of peaks of the raw signal (six peaks). The first mode of each MM-FBG can be identified by the highest peak value, at the wavelengths 835.5 and 859.1 nm for the first and second MM-FBGs, respectively. The spectra wavelength width is approximately 2 nm. The signal obtained from each MM-FBG includes noise, but provided this is not greater than the largest signal peak, the wavelength shift will be determined by the correlation process.

Typical computer screen outputs for correlation signal processing are shown in Fig. 5. Strain measurements at constant

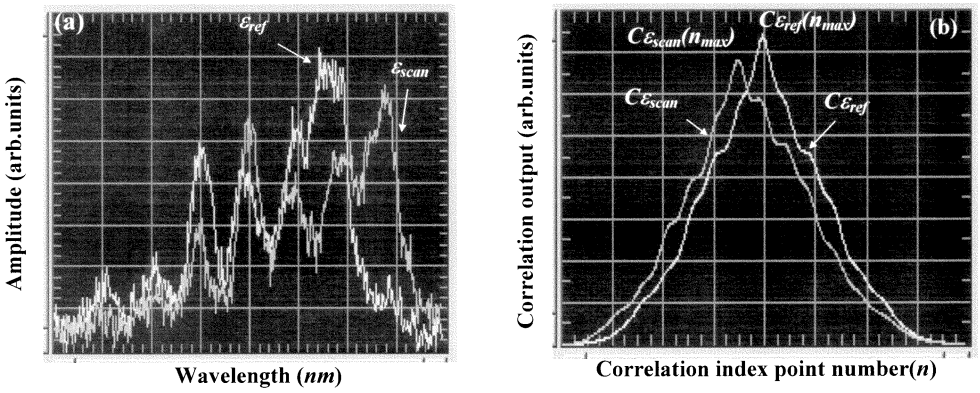

(a) (b)

Fig. 5. Computer screen outputs: (a) raw reference data and raw scanning data and (b) correlation output.

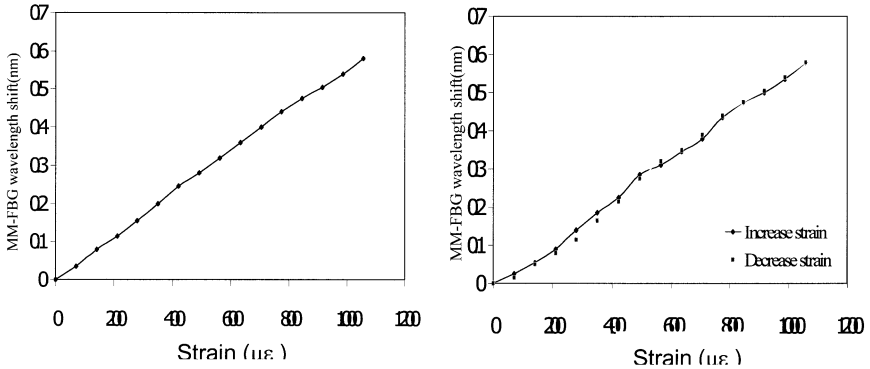

(a) (b)

Fig. 6. Multimode FBG spectrum wavelength shift with axial strain, at room temperature of both MM-FBGs: (a) the first grating and (b) the second grating.

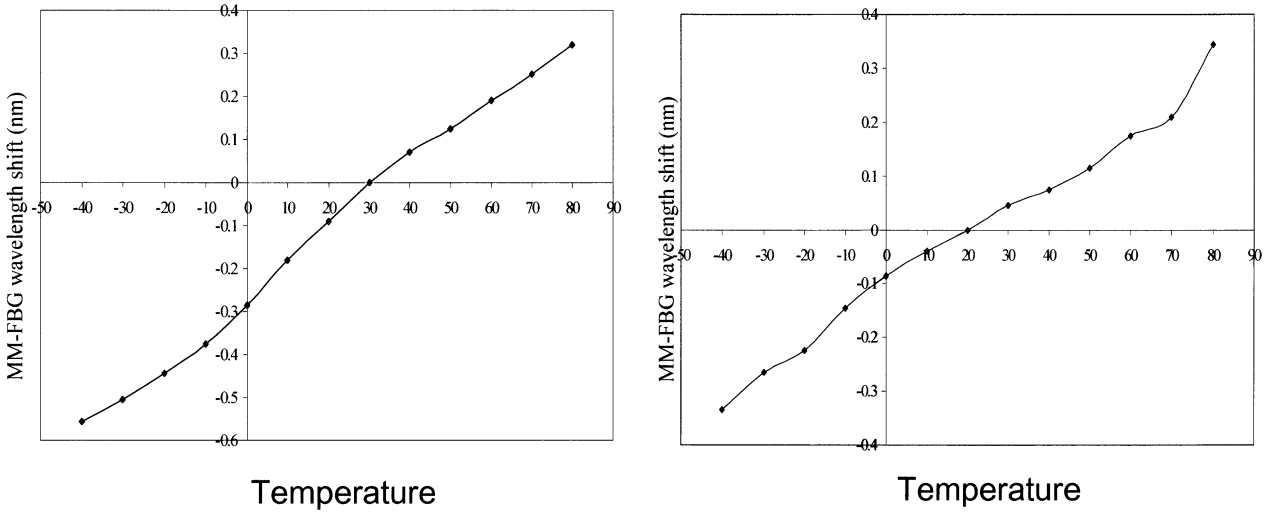

(a) (b)

Fig. 7. Multimode FBG spectrum wavelength shift with temperature, at zero strain, for (a) the first grating and (b) the second grating.

ambient temperature were made as shown in Fig. 5(a). The relationships between MM-FBG wavelength shift and axial strain at room temperature for both MM-FBGs are shown in Fig. 6. As can be seen, there is a reasonably linear relationship. In the experiment, the strain was altered and the reflection of the spectrum measured. The strain coefficient was estimated to be 0.6 pm/$\mu\varepsilon$. This value is comparable with that obtained for conventional Bragg gratings in single-mode fibers. The experimental strain sensitivity for the MM-FBG is 0.55 pm/$\mu\varepsilon$, which is consistent with the estimated value. The repeatability for each strain measurement point was $\pm$0.02 nm wavelength shift (determined by the spectrum analyzer). Hysteresis was small [Fig. 6(b)].

Fig. 7 illustrates the relationship between Bragg grating spectrum wavelength shift and temperature for both of the MM-FBGs. In this experiment, the temperature was varied from $-$40 to 80 °C at constant strain and signal processing and

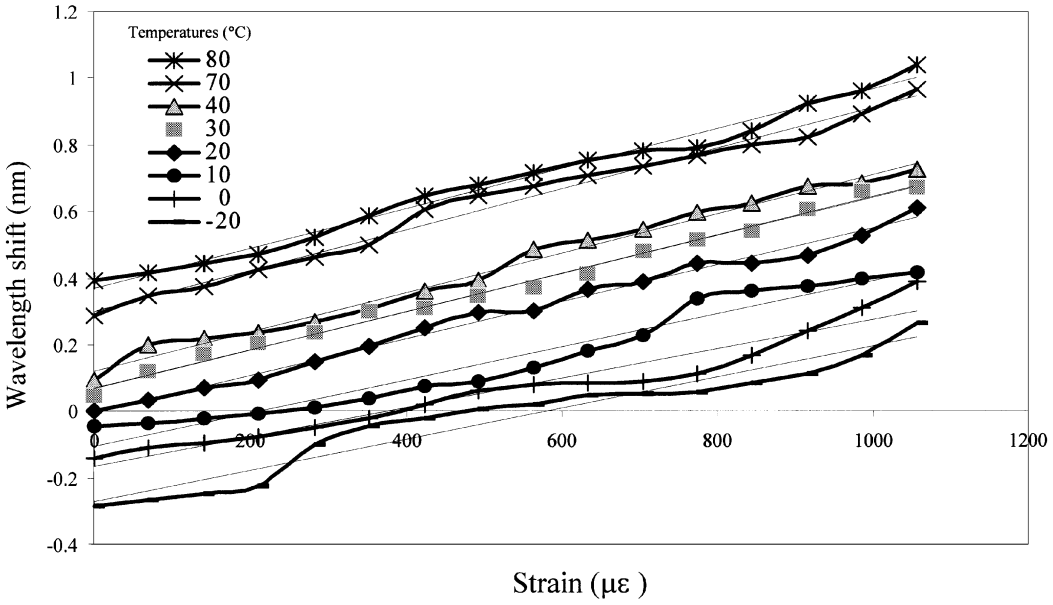

Fig. 8. Strain test at various temperatures.

measurement made as shown in Fig. 3(b). The average temperature sensitivity (between −40 and 80 °C) of the first FBG is 6.8 pm/°C, which is compatible with the predicted value of 7 pm/°C, but the relationship is nonlinear. The repeatability for each temperature measurement point was found to be within a wavelength shift of ±0.03 nm range. For the second FBG, the average temperature sensitivity is approximately 6 pm/°C, which is lower than the predicted value. This may be caused by the buffer coating that could reinforce the fiber and affect the fiber expansion characteristic.

The MM-FBG strain sensitivity to temperature has been investigated by using the second MM-FBG. Axial strain was applied to the fiber using a fiber fixture/drawer that was located in a temperature-controlled chamber. The axial strain was varied from 0 to 1000 $\mu\varepsilon$ by adjusting the micrometer and the temperature was varied from −20 to 80 °C. The results are shown in Fig. 8, with an average temperature coefficient of approximately 7 pm/°C, agreeing with the value from the previous test at zero strain.

IV. Discussion and Conclusions

The method of signal processing using correlation has the major advantage of providing an output for the MM-FBG sensor that is not critically dependent on the power level of the signal, as presented in Fig. 5. A fairly linear characteristic has been obtained for tensile strain from 0 to 1000 $\mu\varepsilon$. The strain sensitivity from the experimental result is in agreement with the estimated value obtained from the SM-FBG mathematical model. The two MM-FBGs, one fabricated by holographic and one by phase mask methods, provided similar strain characteristics, and there was little effect caused by the fiber buffer coating. The temperature characteristic is somewhat nonlinear due to the changing with temperature of many parameters, such as fiber diameter, MM-FBG grating pitch, and reflective index difference between core and cladding of the fiber. However, the average temperature sensitivity of the first MM-FBG, from the experimental result is very close to the predicted value. The second MM-FBG provided slightly lower temperature sensitivity than the predicted value due to the effect of the fiber buffer coating. The strain test at various temperatures provided results in agreement with the previous results. The multimode Bragg grating sensor systems described in this paper are being applied in a power-by-light hydraulic valve monitoring system. The correlation processing method employed may be utilized for MM-FBG optical sensing of many other physical parameters such as pressure and flow-rate.

Acknowledgment

The FBGs were provided by the Department of EEAP, Aston University.

References

[1] J. Lim, Q. P. Yang, B. E. Jones, and P. R. Jackson, "DP-flow sensor using optical fiber Bragg gratings," *Sens. Actuators A*, vol. A2960, pp. 1–7, 2001.

[2] J. Lim, P. R. Jackson, B. E. Jones, K. F. Hale, and Q. P. Yang, "An intrinsically safe optically powered hydraulic valve," in *Proc. 7th Int. Conf. Actuators*, Bremen, Germany, 2000, pp. 216–219.

[3] J. Lim, P. R. Jackson, B. E. Jones, and Q. P. Yang, "Optically powered hydraulic pilot valve using piezoelectric multilayer actuator," *Int. J. Fluid Power*, vol. 2, no. 3, pp. 6–11, 2001.

[4] K. H. Wanser, K. F. Voss, and A. D. Kersey, "Novel fiber devices and sensors based on multimode fiber Bragg gratings," *Proc. SPIE*, vol. 2360, pp. 265–268, 1994.

[5] K. H. Wanser, "Fiber Devices and Sensors Based on Multimode Fiber Bragg Gratings," U.S. Patent 58 482, 1998.

[6] T. V. Djambova and T. Mizunami, "Simultaneous sensing of the temperature and displacement using a multimode fiber Bragg grating," *Jpn. J. Appl. Phys.*, vol. 39, pp. 1566–1570, 2000.

[7] T. Mizunami, T. V. Djambova, T. Niiho, and S. Gupta, "Bragg gratings in multimode and few-mode optical fibers," *J. Lightwave Technol.*, vol. 18, no. 2, pp. 230–235, 2000.

[8] W. Zhao and R. O. Claus, "Optical fiber grating sensors in multimode fibers," *J. Smart Mater. Structure*, vol. 9, pp. 212–214, 2000.

[9] A. Othonos and K. Kalli, *Fiber Bragg Gratings, Fundamentals and Applications in Telecommunications and Sensing*. Boston, MA: Artech House, 1999, pp. 302–337.

[10] R. Kashyap, *Fiber Bragg Gratings*. London, U.K.: Academic, 1999, pp. 409–440.
[11] R. M. Cazo, O. Lisboa, H. T. Hattori, V. M. Schneider, C. L. Barbosa, R. C. Rabelo, and J. L. S. Ferreira, "Experimental analysis of reflected modes in a multimode strained grating," *Microwave Opt. Technol. Lett.*, vol. 28, no. 1, pp. 4–8, 2001.
[12] E. C. Ifeachor and B. W. Jervis, *Digital Signal Processing—A Practical Approach*. New York: Addison-Wesley, 1993, pp. 183–250.

Jirapong Lim received the B.Eng. and M.Eng. degrees in production engineering with a major in industrial automation systems in 1991 and 1996, respectively, from King Mongkut's Institute of Technology, North Bangkok, Thailand. He received the Ph.D. degree in 2001 for work in the field of power-by-light and control-by-light of hydraulic valve systems from the Department of Systems Engineering, Brunel University, Middlesex, U.K.

From 1992 to 1998, he worked in the automation industries and then joined King Mongkut's Institute of Technology as a Lecturer. He currently lectures on industrial measurement and control systems at the same university.

Qingping Yang received the diploma in instrumentation and measurement from Chengdu Aeronautical Polytechnic, China, in 1983. He was awarded a scholarship to study at Brunel University, Middlesex, U.K., in 1998, where he received the Ph.D. degree in 1992.

He was an Assistant Engineer with the Aircraft Structural Strength Research Institute, China. He currently lectures on manufacturing measurement and quality engineering. His research interests include advanced sensors, dimensional metrology, quality engineering, virtual instrumentation, and measurement science. He has published more than 35 papers in these areas.

Barry E. Jones received the D.Sc. degree from the University of Manchester, Manchester, U.K., in 1985.

He has been Professor of manufacturing metrology at Brunel University, Middlesex, U.K., and Director of the Brunel Centre for Manufacturing Metrology (BCMM), since 1986. He holds fellowships of five professional bodies, is author and editor of five books, and has published over 250 papers and articles.

Prof. Jones received a 1995 Metrology for World Class Manufacturing Award as Champions of Metrology. He is a previous Honorary Editor of the *Journal of Physics E: Scientific Instruments* (now *Measurement Science and Technology*) and a past member of the U.K. Council for National Academic Awards.

Phillip R. Jackson received the B.Eng. degree from Edinburgh University, Edinburgh, U.K., and subsequently received the M.Sc. and Ph.D. degrees in industrial measurement and control systems from Brunel University, Middlesex, U.K., in 1993 and 1996, respectively.

He is a Senior Project Engineer at Flight Refuelling Ltd., Wimborne, U.K., working in the field of power-by-light and control-by-light technology for the aerospace industry.